IMPACT EXPERIMENTS ON DRY AND WET SANDSTONE

F. Schaefer [(1)], K. Thoma[(1)] , T. Behner[(1)], S. Nau[(1)], T. Kenkmann[(2)], K. Wünnemann[(2)], Alex Deutsch[(3)], and the MEMIN-Team[(4)]

[(1)] Fraunhofer-Institute for High-Speed Dynamics (Ernst-Mach-Institut, EMI), Eckerstr. 4, 79104 Freiburg, Germany, Email: schaefer@emi.fhg.de, thoma@emi.fhg.de, behner@emi.fhg.de, nau@emi.fhg.de
[(2)] Museum für Naturkunde, Humboldt-Universität Berlin, Invalidenstraße 43, 10115 Berlin, Germany, Email: thomas.kenkmann@museum.hu-berlin.de, kai.wuennemann@museum.hu-berlin.de
[(3)] Institut fuer Planetologie, Westfaelische Wilhelms-Universitaet Muenster, Wilhelm-Klemm-Str. 10, 48149 Muenster, Germany, Email: deutsca@uni-muenster.de *[(4)] see Acknowledgement below*

ABSTRACT

The availability of a new powerful light-gas gun accelerator at the Fraunhofer-Institute for High-Speed Dynamics, Ernst-Mach-Institute (EMI), has triggered a study that investigates the dynamics of impact processes in sandstone. Using this accelerator, crater sizes in the decimetre-range can be obtained, narrowing further the gap between crater sizes obtainable in laboratory and geological impact craters: The smallest impact craters detected on the earth's surface differ in size by roughly two to three orders of magnitude with regards to what can be achieved with the new facility. Hence, the new experimental capabilities enable a more realistic laboratory simulation of geological impact processes.

Two impact cratering experiments on dry and wet sandstone have been performed. This paper provides a description of these impact experiments and the measurements performed including crater size analysis, pressure curve recordings, and high-speed shadowgraphs. The impact cratering experiments reported here are designed to support the comprehensive understanding of the dynamics of impact processes and the quantification of the properties of impact-damaged sandstone. These investigations are performed in the framework of a ***M***ultidisciplinary ***E***xperimental and ***M***odeling ***I***mpact crater research ***N***etwork (***MEMIN***), which was recently established and combines the expertise of geologists, geophysicists, engineers, and modellers [1].

1. TARGET DESCRIPTION

The targets were blocks (1.0 x 1.0 x 0.5 m^3) of sandstone (“Seeberger Sandstein”, Fig. 1), which had a distinct stratified structure (Fig. 2). Its average density amounted to 2.2 g/cm^3. The target material has an average grain size of 0.17 mm and ~18 % porosity (Fig. 3). One of the blocks was put in a water basin for four months and reached a water saturation of 44 vol. % (Fig. 4).

Fig. 1. Sandstone target blocks

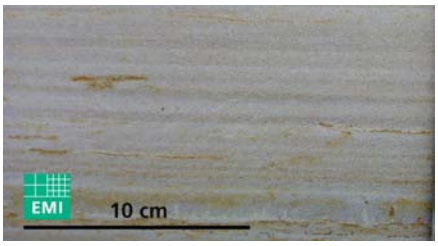

Fig. 2. Stratified target structure

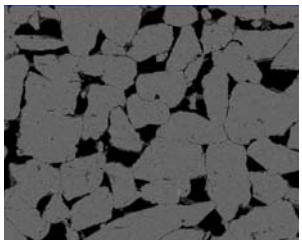
Fig. 3. Microscopic picture of target material, showing sand particles and voids (black)

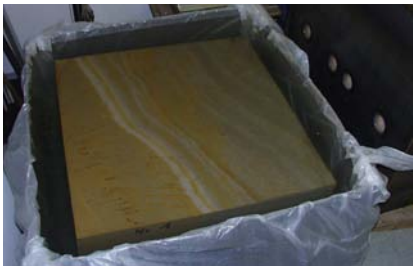
Fig. 4. Watered sandstone block

The strength and elastic modulus are 62.4±2.8 MPa and 14.8±1.4 GPa respectively for the dry sandstone and 47.0±3.7 MPa and 12.1±1.0 GPa for the highly water saturated equivalent.

2. HYPERVELOCITY IMPACT FACILITY

2.1 Working Principle

The accelerator system is based on the two stage light gas gun principle.

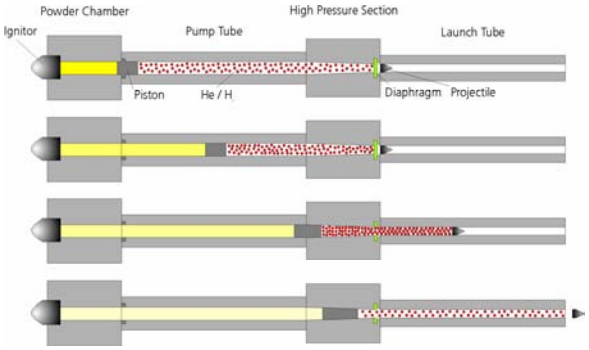

Fig. 5. Working principle of a two-stage light-gas gun

A schematic sketch of the working principle is shown in Fig. 5. The expanding gases of the combusting gun powder drive a plastic piston in the pump tube. The pump tube is filled with a light-weight gas, either Helium (He) or Hydrogen (H). The piston compresses the gas between its leading surface and a thin metal diaphragm located in the high pressure section, which is the joining point between the two gun barrels. This diaphragm prevents the light weight gas in the pump tube from escaping into the launch tube until the gas is compressed to a specific pressure at which the diaphragm is ruptured. Behind the diaphragm is the projectile, embedded in a plastic cylinder (sabot), which is launched by the escaping light-weight gas from the pump tube.

After the projectile exits the launch tube, it enters the blast tank, where the sabot separates from the projectile under action of the residual atmosphere. Before the projectile enters the target chamber, a laser light barrier measurement system determines the velocity of the projectile. Immediately after the velocity measurement, the sabot parts are captured, allowing only the projectile to enter the target chamber. In the target chamber, a high speed framing camera has been integrated to capture shadowgraph images of the impact process. Such guns are used for spacecraft protection applications [2,3] and research related to hypervelocity impacts on geological matter [4].

2.2 Facility description

The facility and the gun are shown in Fig. 6 [5]. The gun is modular, offering a large variety of gun configurations enabling application of launch and pump tubes with different lengths and diameters. The largest gun configuration consists of a 22 m long pump tube, with a caliber of 150 mm, in combination with a 12 m long launch tube of caliber 50 mm. All of the following experimental results refer to this configuration. For an accelerated mass of 150 gr. (sabot + projectile), the current maximum velocity of the gun exceeds 6 km/s. The facility can be operated at atmospheric pressure or evacuated to forevacuum pressures.

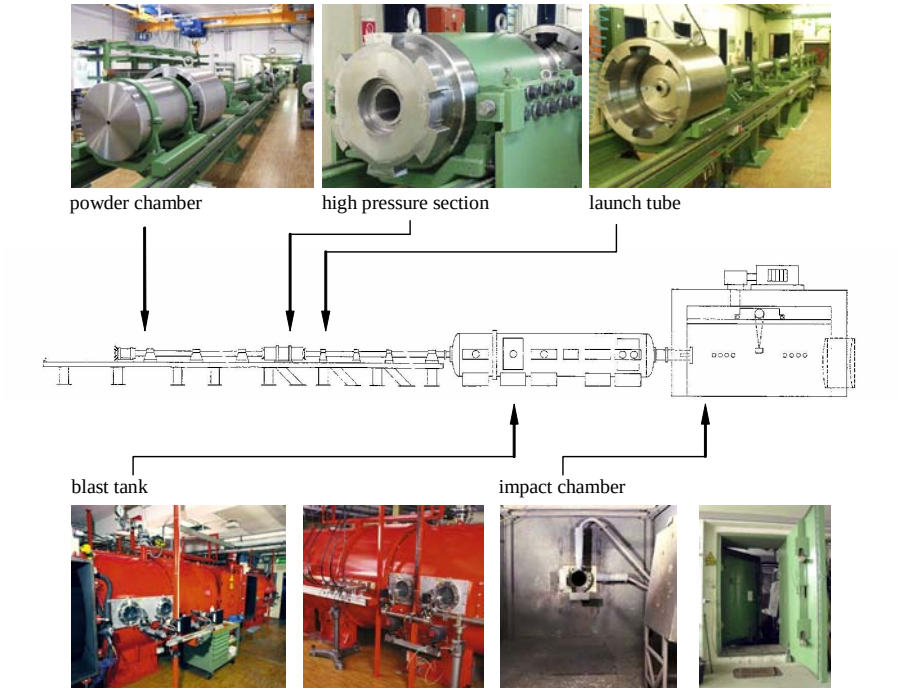

Fig. 6. EMI's two stage light gas gun at proving ground Efringen-Kirchen, south of Freiburg. The upper row shows the launcher system, the lower row the blast tank and the impact chamber with its double access door

3. SET-UP

The set-up is shown in Fig. 7. The blocks were positioned vertically to simulate a vertical impact on flat lying sediments. The target was enclosed in a steel casing, with only the target surface designated for impact left uncovered. Uprange ejecta catchers consisted of fiber boards with an area of 1 m^2 and a 10 cm hole for allowing the projectile to pass. The catchers were placed about 55 cm in front of the target surface. Carbon resistor- and SMD (Surface Mounted Device) resistor shock pressure gauges, manufactured at EMI, were emplaced within the sandstone blocks at a depth of 6 cm beneath the sandstone surface. Two gauges were placed at each lateral side of the target block, and four sensors were placed at the rear side. A 16 channel High Speed Digital Camera was used to image the ejection process in a shadowgraph imaging technique. The camera was placed perpendicular to the shot direction, in the plane of the front target surface. Camera, flash, and transient recorder for the shock pressure gauges were triggered by a trigger foil that was electrically shorted by the impacting projectile during the first tens of nanoseconds of the penetration phase. The shots were performed with the target chamber pre-conditioned to reduced pressure of ca. 0.5 bar.

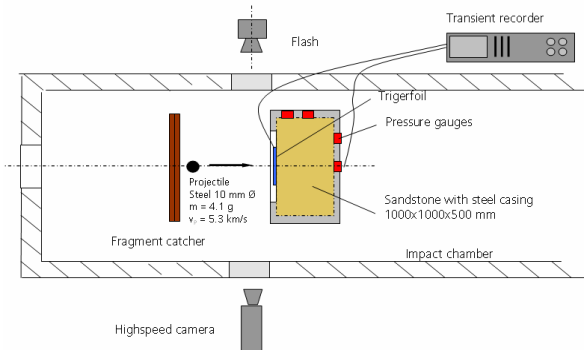

Fig. 7. Experimental set-up

Fig. 8. Target set-up: left: fragment catcher, right: sandstone block

Fig. 9. Right: side of the target block, showing the steel casing and two of the integrated pressure gauges; Left: rear side of the target with 4 gauges integrated

4. IMPACT EXPERIMENTS

Two impact crater experiments were performed with a dry and a water saturated sandstone, respectively. In both cases, the projectile was a 10 mm diameter steel sphere with a mass of 4.1 g. The material specification of the steel was: AISI 4130 Steel, German Industry Standard material number DIN 1.7218. The sabot mass was established at 113 gr., which is relatively high compared to the projectile mass, in order to ensure safe acceleration of the projectile. The impact velocities were ca. 5.3 km/s in both impact experiments (Table 1). In future experiment campaigns, savings on the sabot mass through optimized design can be realized, permitting higher velocities to be attained with the same gun loading parameters.

Table 1 Impact parameters

	dry sandstone (Exp. 2808)	wet sandstone (Exp. 2809)
projectile	Steel 10 mm, 4.1 gr.	Steel, 10 mm, 4.1 gr.
impact velocity	5.34 km/s	5.27 km/s

5. EXPERIMENTAL RESULTS

5.1 Impact Damage

The impact craters were funnel shaped (Fig. 10). The crater in the dry sandstone (Exp. 2808) had an average diameter of 24.3 cm and a depth of 5.6 cm, whereas in the wet sandstone (Exp. 2809) the crater diameter amounted to 28.7 cm and the depth to 4.5 cm (Fig. 11). Volumetrical analyses of the craters based on 3D-scans determined 715 and 1099 cm^3 of excavated material in the dry and wet case, respectively [1]. These results show that the presence of fluid has influenced significantly the cratering process. A wider spall zone

and a shallower crater depth characterize the wet target compared to the dry sandstone.

Fig. 10. Impact crater in wet sandstone - perspective

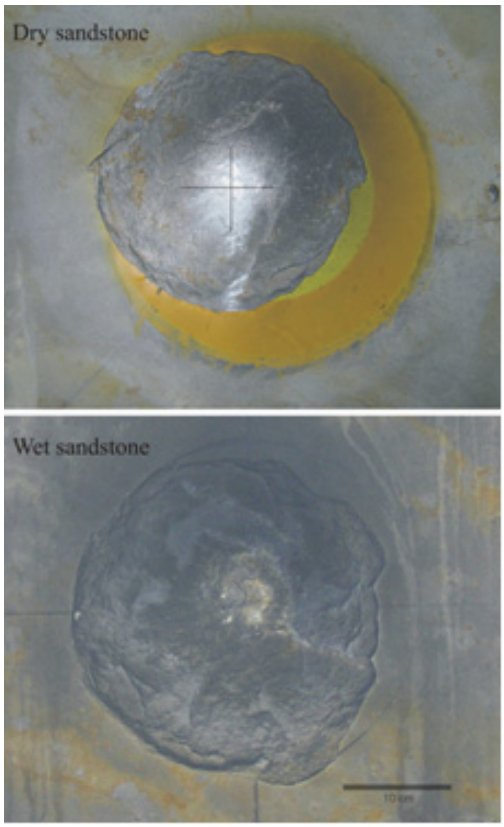

Fig. 11. Impact craters - top view

The uprange ejecta from both targets comprised a wide spectrum of fragment sizes from below 160 µm to above 3 cm. The size distribution had a maximum in the size interval 160-310 µm corresponding to the initial grain size of the sandstone, and in the size range exceeding 2.5 cm, which corresponds to spall fragments. The uprange ejecta caused just minor impact damage in the fragment catcher (Fig. 12), ranging from minor surface erosion to shallow craters with a maximum size of about 1 cm. The main portion of craters produced by the ejecta were located in an area with an outer diameter of about 810 mm (Exp. 2808) and 790 mm (Exp. 2809).

In the impact experiment on the dry sandstone, a single large remnant of the projectile having 69% of the steel projectile mass was recovered from its position in the uprange fragment catcher, at a radial distance of just about 10 cm from the shot-axis. In the impact experiment on the wet sandstone no larger projectile remnants were found, which was most likely due to it passing right through the hole in the fragment catcher.

Fig. 12. Damage from uprange ejecta in fragment catcher in Exp. 2809 (wet sandstone)

5.2 Ejecta velocities

Ejecta velocities were determined from the high-speed shadowgraphs during a time frame of ca. 1.2 ms, shown in Fig. 17 for Exp. 2808 (dry sandstone) and Exp. 2809 (wet sandstone). The shutter time was 180 ns. From the high-speed shadowgraphs it is obvious that most of the ejected matter is concentrated both in the central portion of the cloud and the cone. Further, the digital images suggest higher ejection velocities for the wet sandstone compared to the dry sandstone. The ejecta velocities were determined from the projection of the expanding cone fragments in a plane perpendicular to the target surface, schematically shown in Fig. 13. Thus, the values supplied below refer to the normal components of the ejection velocities. The actual expansion velocities along the cone can be obtained by dividing the supplied values by cos α.

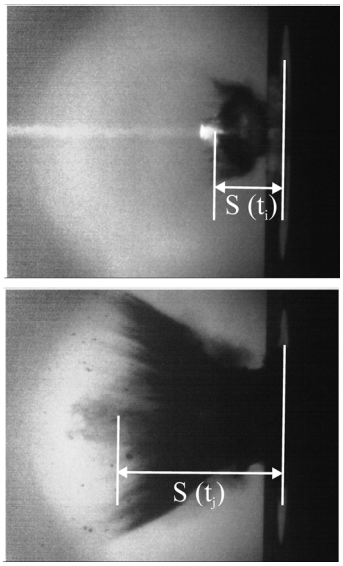

Fig. 13. Determination of ejecta velocities

The mean ejecta velocity perpendicular to the target surface as plotted in Fig. 14 decreases from 2.3-2.4 km s^{-1} in a time frame between projectile encounter and 20 µs afterwards to 0.2-0.3 km s^{-1} after 230-470 µs. On average, the velocities of the ejecta from the wet sandstone are up to 50 % higher than for the dry sandstone. The reason for this behaviour is under investigation. It is believed that the vaporization of the water in the wet sandstone may serve as an additional source of acceleration for the ejecta.

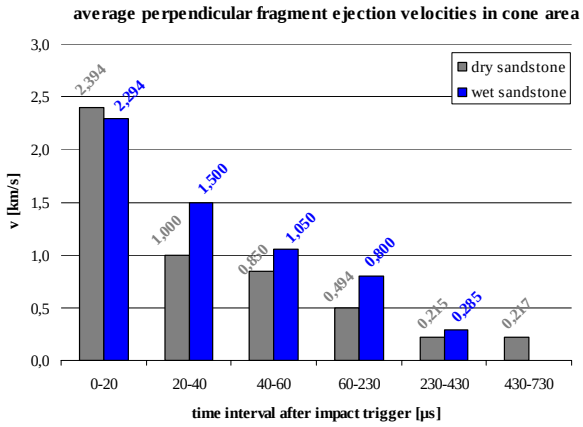

Fig. 14. Average perpendicular fragment ejection velocities for both shots

Ejecta cone angles recorded with high speed cameras are 69.8° and 58° after 1.23 msec in the dry and wet experiments [1].

5.3 Pressure gauge records

Pressure-time profiles recorded with the gauges integrated in the rear side of the target block (K13 for dry sandstone, S4 for wet sandstone, see Fig. 15) have been analyzed. The pressure-time signals are plotted in Fig. 16, where the reference time 0µs corresponds to the impact trigger, the same as was used for the high-speed shadowgraphs. The signal curves are normalized to the maximum pressure signals recorded, because the pressure gauges are currently under calibration at EMI. Thus, only preliminary magnitudes for the peak pressures can presently be provided.

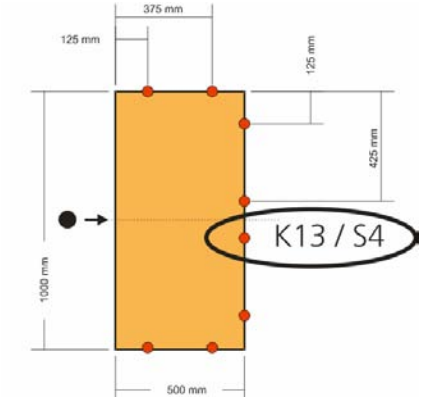

Fig. 15. Pressure gauge locations

As can be seen from Fig. 16, the shape of the signal time curves in both experiments is similar. In both experiments the arrival of the compression wave at the gauge locations occurs about 150 µs after impact trigger. The strong pressure peak is followed by a release wave caused by the reflection of the wave at the rear surface of the target block, starting at ca. 180 µs, and continuing for several 100 microseconds. The preliminary evaluation of the signal amplitudes indicate that the peak pressures measured in the dry sandstone block reach a magnitude of about 5 MPa at about 45 cm from the impact location, while the peak pressures measured in the wet sandstone are about one order of magnitude lower. The reasons for this massive difference are under investigation.

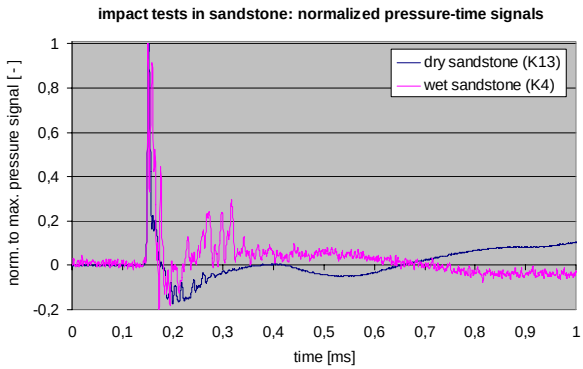

Fig. 16. Normalized pressure-time signals recorded at the rear side of the target blocks, see Fig. 15 (K13: Exp. 2808, S4: Exp. 2809)

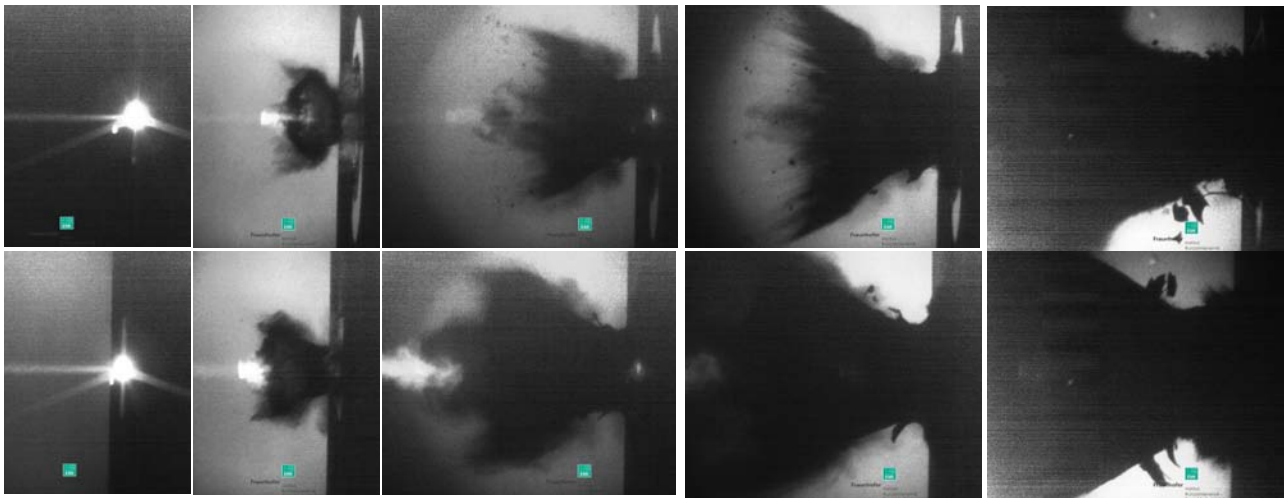

50 ns 80 μs 280 μs 480 μs 1230 μs

Fig. 17. Impact experiment on 0.5 m^3 dry (Exp. 2808, top row) and wet (Exp. 2809, bottom row) sandstone target with a 4.1 g Steel Projectile at 5.3 km/s; High-Speed Digital Shadowgraphs of ejecta cone evolution during initial 1230 μs after impactor encounter with sandstone target.

6. SUMMARY

Ernst-Mach-Institute now possesses a new powerful Light Gas Gun accelerator that is able to generate decimetre-size craters in a sandstone target. The availability of this accelerator offers more realistic opportunities for laboratory simulation of geological impact processes. In this project, which is part of the MEMIN program, the influence of the water content in porous rock vs. dry rock on cratering, shock wave amplitudes, and fragment ejection processes was investigated. It was found that impact into water-saturated sandstone results in shallower but wider craters with larger volumes. It also causes higher ejection velocities of the ejecta. The pressure gauge recordings indicate that the peak pressures at the rear of the sandstone targets are about one order of magnitude lower for the wet sandstone than for the dry sandstone. Analysis of the results is ongoing.

7. ACKNOWLEDGEMENT

The authors would like to acknowledge the contributions of the other members of the MEMIN team to this paper, especially for the mechanical and physical target properties: W. U. Reimold, R.T. Schmitt, L. Hecht (Museum für Naturkunde, Humboldt-Universität Berlin, Germany); U. Yaramanci, S. Mayr, (Abteilung Angewandte Geophysik, Technische Universität Berlin, Germany); C. Grosse (Institut für Werkstoffe im Bauwesen, Universität Stuttgart, Germany); G. Dresen (Projektbereich 3.2, GeoForschungsZentrum Potsdam, Germany); J. Kuder (Fraunhofer EMI, Efringen-Kirchen prooving ground)

8. REFERENCES

1. Kenkmann T., et al., *LPSC XXXVII*, Abs. # 1587, 2006.
2. Schneider E. and Schaefer F., Hypervelocity impact research - acceleration technology and applications *Advances in Space Research*, 28 (2001) pp. 1417-1424
3. Schaefer F., Geyer T., Schneider E., Rott M., and Igenbergs E., Degradation and Destruction of Optical Surfaces by Hypervelocity Impact, *Int. J. Impact Engng.* Vol. 26, 2001, pp 683 - 698
4. Thoma K., Hornemann U., Sauer M., Schneider E., Shock waves - Phenomenology, experimental, and numerical simulation, *Meteoritics & Planetary Science* 40, Nr. 9/10, 1283-1298, 2005
5. Junginger M., Schmolinske E., Performance Tests of a new Two Stage Light Gas Gun at the Ernst-Mach-Institut, Proc. 53rd Meeting of the Aeroballistic Range Association, October 21-25, 2002, Sendai, Japan